

ANL/CAM/CP--88736

The submitted manuscript has been authored by a contractor of the U. S. Government under contract No. W-31-109-ENG-38. Accordingly, the U. S. Government retains a nonexclusive, royalty-free license to publish or reproduce the published form of this contribution, or allow others to do so, for U. S. Government purposes.

CONF-951205--4

RECEIVED

TWO INTERESTING FEATURES IN THE INFRARED AND RAMAN SPECTRA OF THE 12K ORGANIC SUPERCONDUCTOR  $\kappa$ -(ET)<sub>2</sub>Cu[N(CN)<sub>2</sub>]Br. FEB 18 1996

OSTI

J. E. ELDRIDGE AND Y. XIE  
 Department of Physics, University of British Columbia, Vancouver, B.C., V6T 1Z1, Canada.

H. H. WANG, J. M. WILLIAMS, A. M. KINI, AND J. A. SCHLUETER  
 Chemistry and Materials Science Division, Argonne National Laboratory, Argonne, IL 60439, USA

**Abstract** Two of the larger features in the infrared conductivity spectra of  $\kappa$ -(ET)<sub>2</sub>Cu[N(CN)<sub>2</sub>]Br are analysed and one is reassigned with the aid of infrared and Raman spectra of isotopically-substituted compounds.

Figure 1 shows the infrared conductivity of ET copper dicyanamide bromide at various temperatures<sup>1</sup>. One can see that as the material is cooled the far-infrared intraband electronic conductivity, due to the free carriers, grows at the expense of the mid-infrared interband conductivity. This paper, however, is not concerned with this aspect of the spectrum but rather with two of the larger vibrational features.

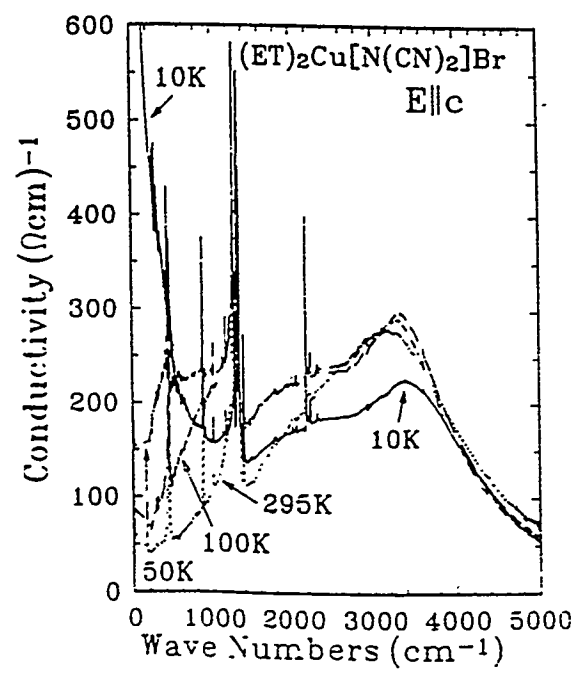


FIGURE 1 The infrared conductivity as a function of temperature.

The first is the large resonance near  $1300\text{ cm}^{-1}$ , correctly assigned to  $\nu_3(A_g)$  but which we will show has changed its nature in this solid, and the second is the sharp line near  $880\text{ cm}^{-1}$ ; which we will show has consistently been misassigned.

### THE $1300\text{ cm}^{-1}$ RESONANCE

This large resonance could have been either  $\nu_2(A_g)$  or  $\nu_3(A_g)$ , both of which are shown in Fig. 2 and which involve the vibration of the same two carbon pairs, but with a  $180^\circ$  phase difference in the case of  $\nu_2(A_g)$ . The reason that these totally-symmetric Raman active vibrations are also infrared active, is the well-known vibronic mechanism whereby charge is transferred between molecules, which are arranged in dimer pairs, as they vibrate out of phase with each other. The size of the molecule depends on the amount of charge it has and therefore the charge will oscillate between the two molecules as they alternately expand and contract. This produces an infrared activity for radiation with the electric field vector polarized *perpendicular* to the molecular plane.

We have recently published a comprehensive analysis of all of the in-plane vibrations of the ET molecule<sup>2</sup>. There are 72 fundamental intramolecular ("internal") normal modes, distributed among the  $D_{2h}$  (planar) symmetry species as follows:

$$\Gamma(D_{2h}) = 12A_g + 6B_{1g} + 7B_{2g} + 11B_{3g} + 7A_u + 11B_{1u} + 11B_{2u} + 7B_{3u} \quad (1)$$

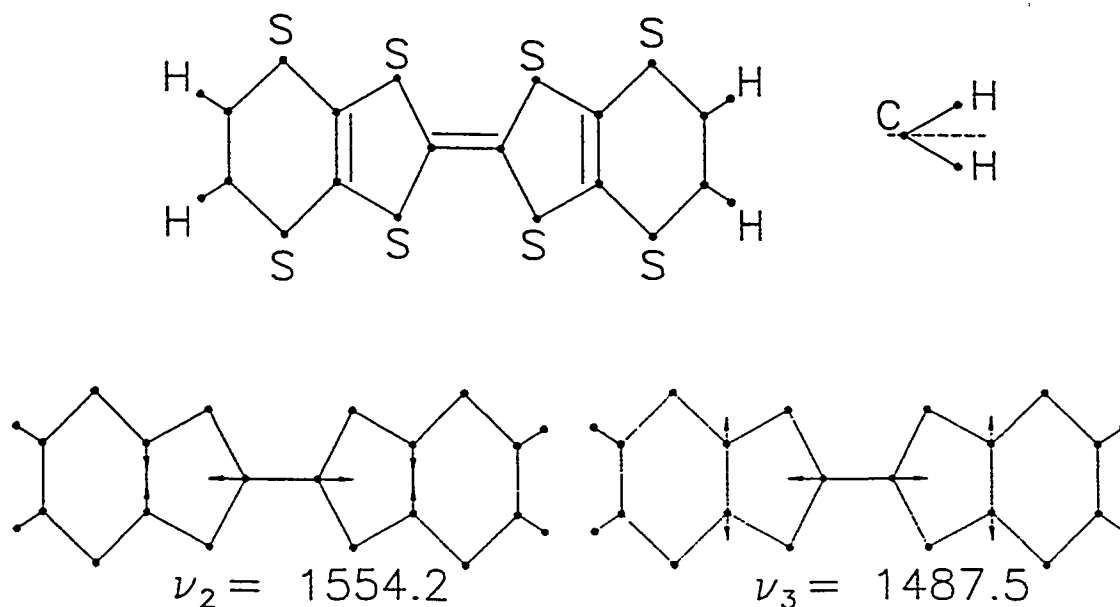


FIGURE 2 The ET molecule and the  $\nu_2(A_g)$  and  $\nu_3(A_g)$  normal vibrations.

The frequencies of these modes change when the mass of the atoms involved changes (the *isotope* effect) or when the charge on the molecule changes (the *ionicity* effect) or when the vibration is coupled to the charge transfer (the *electron-phonon* effect). Figure 3 shows the isotopic analogs we used in the analysis<sup>2</sup> of ET and Table 1 shows the agreement we obtained between the calculated and observed frequencies and isotopic frequency shifts for the first four A<sub>g</sub> modes. One can see that with <sup>13</sup>C at only the central pair sites, both  $\nu_2$ (A<sub>g</sub>) and  $\nu_3$ (A<sub>g</sub>) give 30 cm<sup>-1</sup> shifts while with <sup>13</sup>C at the inner six sites both modes have twice the shift or approximately 60 cm<sup>-1</sup>. This shows that in ET both of these modes involve the central carbon atom pair and the inner-ring carbon atom pairs fairly equally.

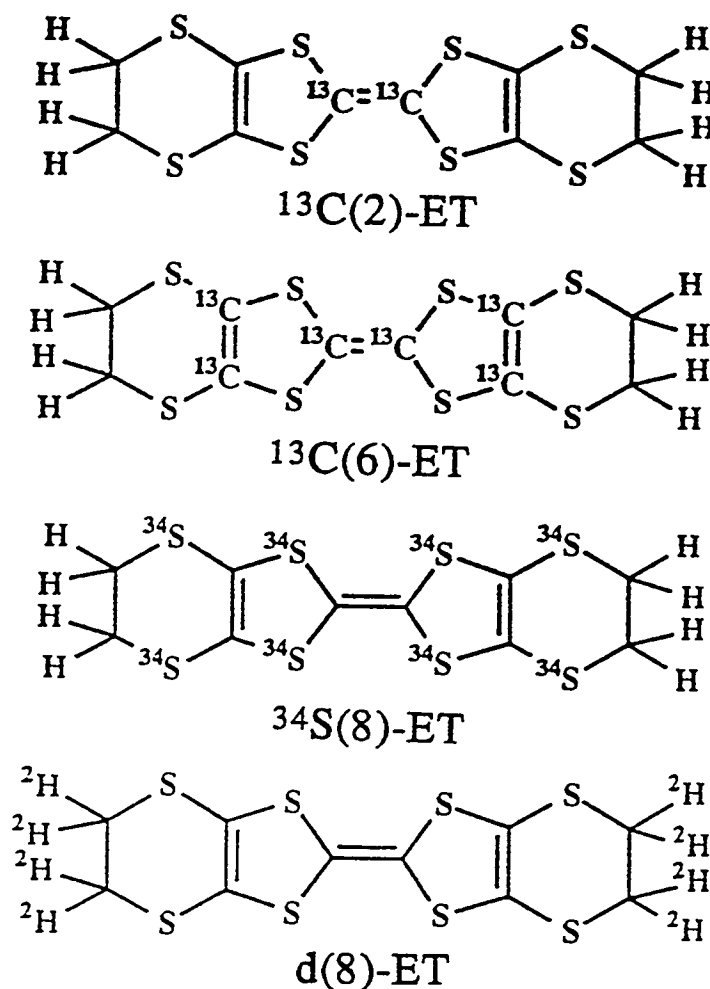


FIGURE 3 The four isotopic analogs of ET used in this study.

TABLE 1 Calculated and observed frequencies and isotopic frequency shifts  
 of the first four totally-symmetric modes.

		$\nu_1(A_g)$	$\nu_2(A_g)$	$\nu_3(A_g)$	$\nu_4(A_g)$
$\nu$ $\text{cm}^{-1}$	CALC.	2941	1554	1488	1413
	OBS.	2920	1551	1493	1408
$\Delta\nu$ $^{13}\text{C}(2)$	CALC.	0	-27	-33	-1
	OBS.	0	-29	-28	0
$\Delta\nu$ $^{13}\text{C}(6)$	CALC.	0	-60	-58	-1
	OBS.	0	-65	-56	0
$\Delta\nu$ $^{34}\text{S}(8)$	CALC.	0	0	-1	0
	OBS.	0	-2	0	0
$\Delta\nu$ $^2\text{H}(8)$	CALC.	-788	0	0	-363
	OBS.	-773	0	+1	-292

Consider now  $\nu_2(A_g)$ . Table 2 lists both Raman and infrared data. In the Raman data are listed the ionicity shift in going from ET to  $(\text{ET})_2\text{Cu}[\text{N}(\text{CN})_2]\text{Br}$  and then the  $60 \text{ cm}^{-1}$  shift, mentioned above, in the  $^{13}\text{C}(6)$  compound. In the infrared spectra, however, after the electron-phonon shift, one sees that in the  $^{13}\text{C}(2)$  compound *there is no  $30 \text{ cm}^{-1}$  negative shift* but rather a slightly positive one, whereas in the  $^{13}\text{C}(6)$  compound the full  $60 \text{ cm}^{-1}$  shift is observed. This means that in the conducting solid  $\nu_2(A_g)$  has changed its nature and *now involves only the inner-ring carbon pair* as drawn in Fig. 4. Figure 5 shows the spectra in question and the features due to  $\nu_2(A_g)$  may be observed.

INFRARED AND RAMAN SPECTRA OF  $(\text{ET})_2\text{Cu}[\text{N}(\text{CN})_2]\text{Br}$

TABLE 2 Experimental infrared and Raman data for  $\nu_2(A_g)$  in ET and  $(\text{ET})_2\text{Cu}[\text{N}(\text{CN})_2]\text{Br}$ . Frequencies and frequency shifts are listed and labelled.

$\nu_2(A_g)$

**RAMAN**

ET	$^{13}\text{C}(2)\text{-ET}$	$^{13}\text{C}(6)\text{-ET}$	$(\text{ET})_2^+\text{Cu}[\text{N}(\text{CN})_2]\text{Br}^-$	$^{13}\text{C}(6)\text{-}\kappa\text{-}(\text{ET})_2^+\text{Cu}[\text{N}(\text{CN})_2]\text{Br}^-$
1551	1522 (-29)	1486 (-65)	1496 (-55)	1436 (-60)
	isotope	isotope	ionicity	isotope

**INFRARED  $E_{1g}$**

$(\text{ET})_2^+\text{Cu}[\text{N}(\text{CN})_2]\text{Br}^-$	$^{13}\text{C}(2)\text{-}\kappa\text{-}(\text{ET})_2^+\text{Cu}[\text{N}(\text{CN})_2]\text{Br}^-$	$^{13}\text{C}(6)\text{-}\kappa\text{-}(\text{ET})_2^+\text{Cu}[\text{N}(\text{CN})_2]\text{Br}^-$
1480 (-16)	1485 (+5)	1419 (-61)
1472 (-24)	1474 (+2)	1414 (-58)
electron-phonon	isotope	isotope

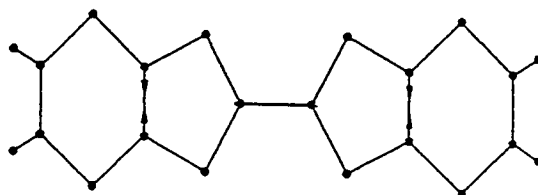


FIGURE 4 The atomic displacements in  $\nu_2(A_g)$  in the conducting solid  $(\text{ET})_2\text{Cu}[\text{N}(\text{CN})_2]\text{Br}$ . Notice that only the inner-ring carbon atom pair is vibrating and not the central pair.

Abstracts: 100-104  
 Equations: 1

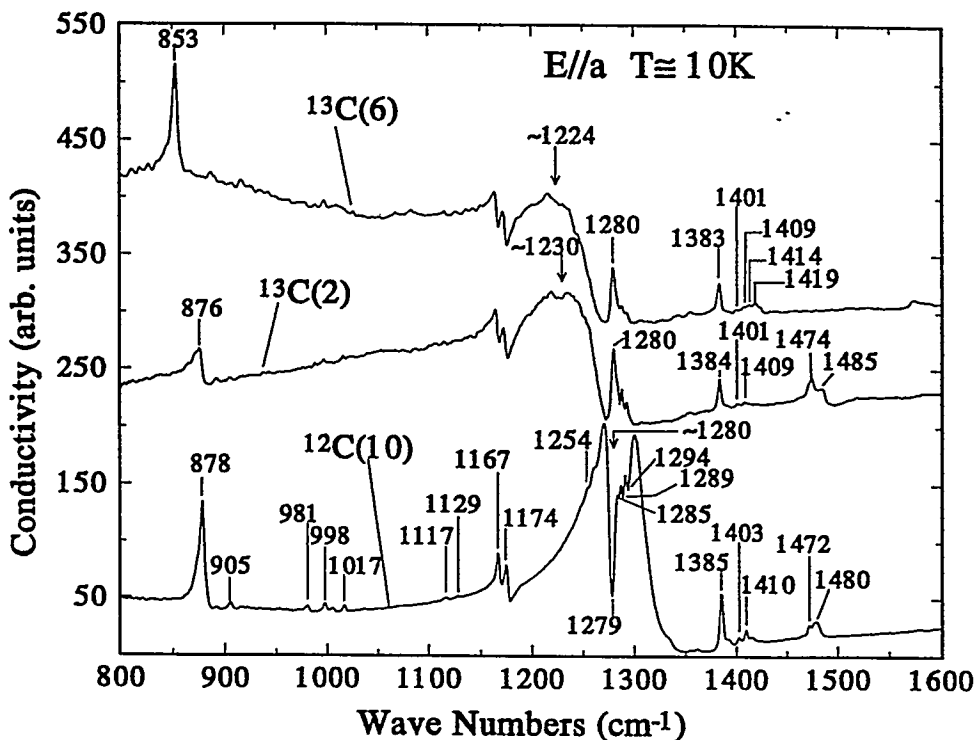


FIGURE 5 The 10K infrared conductivity for EIIa, obtained from a Kramers-Kronig analysis of the reflectivity, of natural  $\kappa$ -(ET) $_2^+$ Cu[N(CN) $_2$ ]Br $^-$ , together with those of the two compounds with  $^{13}\text{C}$  isotopic substitutions. Not all of the features in these latter spectra have been labelled. The  $^{13}\text{C}$  spectra have been offset for clarity.

Similarly consider now  $\nu_3(A_g)$ . Table 3 lists the appropriate data. Comparing the infrared isotope shifts in this case one sees that for the  $^{13}\text{C}(2)$  compound the observed  $50\text{ cm}^{-1}$  shift is almost equal to the full  $56\text{ cm}^{-1}$  shift seen in the  $^{13}\text{C}(6)$  compound. This means that this mode has also changed its nature, presumably because of the very strong electron-phonon coupling, and now consists of the vibration of only the central carbon pair as drawn in Fig.6. The intense broad infrared feature due to  $\nu_3(A_g)$  may also be seen in Fig.5 where it is complicated by the presence of the interacting sharp  $\nu_5(A_g)$  quartet with the strongest line near  $1280\text{ cm}^{-1}$ . These data are being published in more detail elsewhere<sup>3</sup>.

INFRARED AND RAMAN SPECTRA OF  $\kappa$ -(ET)<sub>2</sub>Cu[N(CN)<sub>2</sub>]Br

TABLE 3 Experimental infrared and Raman data for  $\nu_3(A_g)$  in ET and  $\kappa$ -(ET)<sub>2</sub>Cu[N(CN)<sub>2</sub>]Br. Frequencies and frequency shifts are listed and labelled.

$\nu_3 (A_g)$

RAMAN

ET	<sup>13</sup> C(2)- ET	<sup>13</sup> C(6)- ET	(ET) <sub>2</sub> <sup>+</sup> Cu[N(CN) <sub>2</sub> ] Br <sup>-</sup>	<sup>13</sup> C(6)- $\kappa$ - (ET) <sub>2</sub> <sup>+</sup> Cu[N(CN) <sub>2</sub> ]Br <sup>-</sup>
1494	1465 (-28)	1437 (-56)	1468 (-25)	1415 (-53)
	isotope	isotope	ionicity	isotope

INFRARED  $E_{1g}$

(ET) <sub>2</sub> <sup>+</sup> Cu[N(CN) <sub>2</sub> ]Br <sup>-</sup>	<sup>13</sup> C(2)- $\kappa$ - (ET) <sub>2</sub> <sup>+</sup> Cu[N(CN) <sub>2</sub> ]Br <sup>-</sup>	<sup>13</sup> C(6)- $\kappa$ - (ET) <sub>2</sub> <sup>+</sup> Cu[N(CN) <sub>2</sub> ]Br <sup>-</sup>
~1280 (-188)	~1230 (-50)	~1224 (-56)
electron-phonon	isotope	isotope

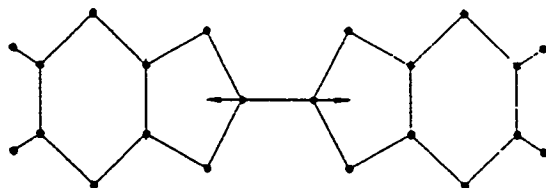


FIGURE 6 The atomic displacements in  $\nu_3(A_g)$  in the conducting solid  $\kappa$ -(ET)<sub>2</sub>Cu[N(CN)<sub>2</sub>]Br. Notice that only the central carbon atom pair is vibrating and not those in the inner ring.



$\kappa$ -(ET)<sub>2</sub><sup>+</sup>Cu[N(CN)<sub>2</sub>]Br<sup>-</sup>, which is twice that observed for  $\nu_3$ (A<sub>g</sub>). The next,  $\nu_7$  (A<sub>g</sub>), is not a serious candidate since it involves the hydrogen atoms, which the infrared data clearly dispute. The next two,  $\nu_{48}$ (B<sub>2u</sub>) and  $\nu_{49}$ (B<sub>2u</sub>) both have the correct frequency and isotope shifts, which is why we originally assigned the feature to  $\nu_{49}$ (B<sub>2u</sub>) but there is no reason for these modes, which are infrared active, to be so strong in the Raman spectrum.

TABLE 4 Experimental frequencies and shifts of the "880 cm<sup>-1</sup>" feature in  $\kappa$ -(ET)<sub>2</sub><sup>+</sup>Cu[N(CN)<sub>2</sub>]Br<sup>-</sup> together with the calculated frequencies and shifts of modes which have approximately the same frequency in neutral ET.

**$\kappa$ -(ET)<sub>2</sub><sup>+</sup>Cu[N(CN)<sub>2</sub>]Br<sup>-</sup>**

**EXPERIMENTAL**

	Natural	<sup>13</sup> C(2)	<sup>13</sup> C(6)	<sup>34</sup> S(8)	<sup>2</sup> H(8)
	$\nu$	$\Delta\nu$	$\Delta\nu$	$\Delta\nu$	$\Delta\nu$
INFRARED	878	-2	-25	-4	+7
Ella					
RAMAN	889	-1 <sup>a</sup>	-26	-3 <sup>a</sup>	-8 <sup>a</sup>

**ET**

**CALCULATED**

$\nu_6$ (A <sub>g</sub> )	983	-1	-32	-6	-6
$\nu_7$ (A <sub>g</sub> )	918	0	-1	-1	-188
$\nu_{48}$ (B <sub>2u</sub> )	904	-7	-25	-7	-2
$\nu_{49}$ (B <sub>2u</sub> )	890	-20	-27	-5	-2
$\nu_{60}$ (B <sub>3g</sub> )	889	-2	-26	-6	-4

<sup>a</sup> very weak feature in neutral ET

Our best guess, therefore, is the last candidate,  $\nu_{60}(B_{3g})$ . It is normally Raman active, and is drawn below in Fig. 8. It involves the inner-ring carbon atom pairs. The lower part of Fig. 8 shows the molecular arrangement in a  $\kappa$ -phase material, where the lines represent the *end* views of the molecules arranged in dimers with alternating orientation. The reason for the infrared activity of this mode may be as follows. If adjacent molecules in a dimer are oscillating out of phase in the  $\nu_{60}(B_{3g})$  mode, then their orbital overlap is changing and in a  $\kappa$ -phase material this may cause charge to transfer from one dimer to an adjacent dimer, producing the dipole needed for infrared activity. We have also assigned other infrared features to  $B_{3g}$  modes<sup>3</sup>.

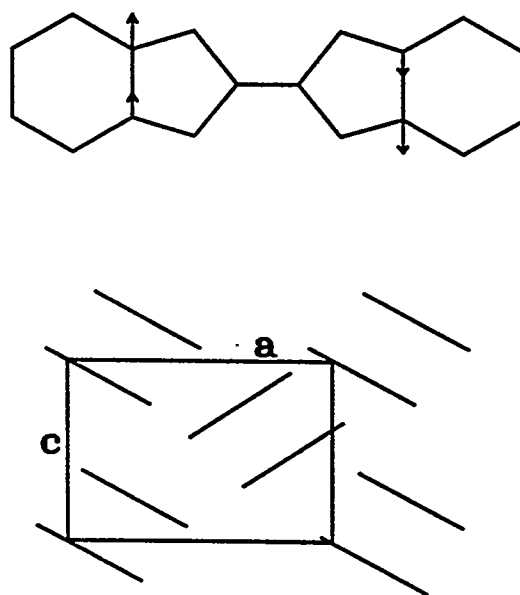


FIGURE 8 Top: An approximate representation of the  $\nu_{60}(B_{3g})$  normal mode. Bottom: A sketch of the unit cell in the *ac* plane showing the end views of the molecular dimers (i.e. their long axes are normal to this *ac* plane).

## REFERENCES

1. J. E. Eldridge, K. Kornelsen, H. H. Wang, J. M. Williams, A. V. Strieby Crouch and D. M. Watkins, *Solid State Commun.*, **79**, 583 (1991).
2. J. E. Eldridge, C. C. Homes, J. M. Williams, A. M. Kini, and H. H. Wang, *Spectrochimica Acta*, **51A**, No. 6, 947 (1995).
3. J. E. Eldridge, Y. Xie, H. H. Wang, J. M. Williams, A. M. Kini, and J. A. Schlueter, *Spectrochimica Acta*, **52A**, No. 1, (Jan. 1996).

## DISCLAIMER

This report was prepared as an account of work sponsored by an agency of the United States Government. Neither the United States Government nor any agency thereof, nor any of their employees, makes any warranty, express or implied, or assumes any legal liability or responsibility for the accuracy, completeness, or usefulness of any information, apparatus, product, or process disclosed, or represents that its use would not infringe privately owned rights. Reference herein to any specific commercial product, process, or service by trade name, trademark, manufacturer, or otherwise does not necessarily constitute or imply its endorsement, recommendation, or favoring by the United States Government or any agency thereof. The views and opinions of authors expressed herein do not necessarily state or reflect those of the United States Government or any agency thereof.